Impact of heterogeneous nuclear ribonucleoprotein A/B subtype overexpression on the expression of cancer stem cell markers CD133 and CD44 and cellular proliferation capacity

Meng Wang[1], Xian Wang[2], Yaping Cui[1], Xing Wen[1*]

[1] Center of Gastrointestinal and Minimally Invasive Surgery, Department of General Surgery, The Third People's Hospital of Chengdu, Affiliated Hospital of Southwest Jiaotong University & The Second Affiliated Hospital of Chengdu, Chongqing Medical University, Chengdu, 610031, China

[2] Department of Anorectal, The Third People's Hospital of Chengdu, Affiliated Hospital of Southwest Jiaotong University & The Second Affiliated Hospital of Chengdu, Chongqing Medical University, Chengdu, 610031, China

ARTICLE INFO

ABSTRACT

The occurrence and progression of intestinal cancer are complex, multifactorial processes in which tumor stem cells are believed to play a crucial role. An in-depth understanding of their molecular mechanisms holds imperative clinical significance for improving intestinal cancer treatment. HT-29 and HCT116intestinal cancer cell lines were utilized as research models. The experimental group (group E) and control group (group C) were established by transfecting the hnRNPA1 subtype and empty vector, respectively. The expression (EP) levels of hnRNPA1 and changes in Wnt/β-catenin signaling-related markers were evaluated using techniques such as RNA extraction, reverse transcription reactions, real-time quantitative PCR (RT qPCR), and protein extraction. The EP of tumor stem cell markers CD133 and CD44 was assessed using immunohistochemistry. Additionally, cell invasion assays, scratch assays, and cell counting kit-8 (CCK-8) proliferation assays were conducted. Furthermore, a mouse tumor model was established to observe the growth of tumors in both groups. overexpression (OP) of hnRNPA1 in group E greatly increased the protein EP levels of β-catenin, Axin2, and Cyclin D1 and exhibited a higher positivity rate for CD133 and CD44. The invasive, migratory, and proliferative abilities of cells in group E were notably enhanced, and tumor growth was observably faster versus group C. OP of hnRNPA1 was closely associated with the activation of Wnt/β-catenin signaling and promoted the proliferation and invasive capacity of tumor cells. hnRNPA1 played an imperative role in intestinal cancer stem cells.

Introduction

Intestinal cancer is a common malignant tumor that originates from the epithelial cells of the colon or rectum and is one of the leading causes of cancer-related deaths worldwide. The progression of intestinal cancer typically involves tumor initiation, growth, invasion, and metastasis. Tumor stem cells, which represent a small subset of cells with self-renewal and multi-lineage differentiation capabilities, play a crucial role in the development and progression of intestinal cancer. Tumor stem cells possess the ability to self-renew, continuously generating tumor cells, thereby contributing to sustained tumor growth (1,2). Furthermore, they exhibit multi-lineage differentiation potential, giving rise to different types of tumor cells, thus increasing tumor heterogeneity. The presence of tumor stem cells holds significant implications for the treatment and prognosis of intestinal cancer. Due to their drug resistance and robust survival capabilities, conventional treatment methods often fail to completely eliminate tumor stem cells, leading to tumor recurrence and metastasis. Therefore, studying the characteristics and regulatory mechanisms of intestinal cancer stem cells is of paramount importance in developing novel therapeutic strategies targeted at these cells (3,4).

Heterogeneous nuclear ribonucleoproteins (hnRNPs) are a highly conserved class of RNA-binding proteins that play imperative roles in processes such as gene transcription, RNA processing, transport, and translation. Recent research has indicated that hnRNPs also play major roles in tumor growth, progression, and treatment. Among the hnRNPs family, hnRNPA1 is one of the most extensively studied subtypes, participating in various cellular activities including transcription, RNA splicing, transport, and translational regulation (5,6). In tumors, the hnRNPA1 subtype was closely associated with tumor cell proliferation, metastasis, and prognosis. The expression (EP) level of the hnRNPA1 subtype is significantly upregulated in intestinal cancer (7), promoting proliferation, metastasis, and invasion of intestinal cancer cells. The overexpression (OP) of the hnRNPA1 subtype can promote tumor cell proliferation and metastasis through various mechanisms. For example, it can regulate the EP of several key cancer-related genes such as MYC, Cyclin D1, and BCL-XL,

thereby promoting the proliferation of intestinal cancer cells (8-10). Wnt/β-catenin signaling is a widely involved pathway in cellular processes and also plays a crucial role in tumor cell proliferation and metastasis. Under normal conditions, Wnt/β-catenin signaling remains inactive, while its activation in tumor cells promotes tumor cell proliferation and metastasis (11,12). Studies have indicated that the hnRNPA1 subtype is involved in the regulation of Wnt/β-catenin signaling, thereby influencing tumor cell proliferation and metastasis (13). Specifically, the hnRNPA1 subtype can enhance the nuclear translocation and stability of β-catenin, thereby increasing the activity of Wnt/β-catenin signaling. Additionally, the hnRNPA1 subtype can regulate the EP of multiple genes related to Wnt/β-catenin signaling. Hence, there is a close relationship between the hnRNPA1 subtype and Wnt/β-catenin signaling, both of which participate in tumor cell proliferation and metastasis. Studies have noted that OP of the hnRNPA1 subtype in tumor cells can promote the activity of Wnt/β-catenin signaling, thus enhancing tumor cell proliferation and metastatic potential (14,15). Thus, targeting the regulation of the hnRNPA1 subtype and Wnt/β-catenin signaling may be an effective strategy for treating tumors.

CD133 and CD44 are tumor stem cell markers, and their EP levels are widely utilized for the identification and isolation of tumor stem cells. In this experiment, the EP levels of CD133 and CD44 were studied to explore the impact of hnRNPAB subtype OP on tumor stem cells in intestinal cancer cells (16). This work aimed to demonstrate the role of the hnRNPAB subtype in intestinal cancer cells, study the EP levels of CD133 and CD44, as well as cell proliferation capacity, to reveal its impact on intestinal cancer. It contributes to a deeper understanding of the characteristics and molecular mechanisms of the stem cell population within intestinal cancer cells and provides new therapeutic targets for the treatment of intestinal cancer.

Materials and Methods

Experimental cell lines, animals, consumables, and equipment

Human intestinal cancer HT-29 and HCT116 cell strains were purchased from Shanghai Guandao Biotechnology Co., Ltd. The hnRNPA1 OP lentivirus packaging and negative control virus were constructed by Beijing Micro-helix Gene Technology Co., Ltd. Eighteen male SPF-grade mice were purchased from Nanjing Biorn Biotechnology Co., Ltd., with an experimental animal license number: 202202155Z. This experiment had been approved by the ethics committee of the Affiliated Hospital of Southwest Jiaotong University & the Second Affiliated Hospital of Chengdu and was in accordance with the standards for the management and use of laboratory animals.

Dulbecco's modified Eagle's medium (DMEM) culture medium (Shanghai Hongming Biotechnology Co., Ltd.); phosphate buffer saline solution (PBS, Wuhan Procell Life Technology Co., Ltd.); radioimmunoprecipitation assay (RIPA) buffer, enhanced chemiluminescence (ECL) detection reagent (Nanjing Senbeijia Biotechnology Co., Ltd.); bicinchoninic acid (BCA) assay kit (Shanghai Jining Industrial Co., Ltd.); immunohistochemistry kit, cell counting kit-8 (CCK-8) assay kit (Shanghai Enzyme-linked Biotechnology Co., Ltd.); polyvinylidene fluoride (PVDF) membrane (Central South Construction Membrane Struc-

ture Group Co., Ltd.); Tris buffered saline Tween (TBST) buffer (Shenzhen Doudian Biotechnology Co., Ltd.); hnRNP A1 primary and secondary antibodies (rabbit polyclonal antibody) (Abcam); 0.25% trypsin solution (Hangzhou Putai Biotechnology Co., Ltd.); 0.1% Prussian blue staining solution (Shanghai Shangbao Biotechnology Co., Ltd.); CD133-FITC antibody, CD44-PE antibody (Beijing Tonglihaiyuan Biotechnology Co., Ltd.); Transwell chamber (Wuhan Boyuan Biotechnology Co., Ltd.); centrifuge, constant temperature incubator (Hunan Kaida Scientific Instrument Co., Ltd.); inverted microscope (Shanghai Wumo Optical Instrument Co., Ltd.); microplate reader (Beijing Perlong Technology Co., Ltd.); ultra-low temperature freezer (Shanghai Beiyin Biotechnology Co., Ltd.); PCR instrument, orbital shaker (Shanghai Qiqian Electronic Technology Co., Ltd.); flow cytometer (Beijing Image Trade Co., Ltd.); polyacrylamide gel electrophoresis apparatus (Nanjing GenScript Biotechnology Co., Ltd.).

Experimental grouping

The intestinal cancer cell lines HT-29-hnRNPA1 and HCT116-hnRNPA1 were designated as the experimental groups, while HT-29-NC and HCT116-NC were designated as the control groups.

Lentivirus transfection experiment

In Lenti-X 293T cells, lentiviral packaging was performed using the calcium phosphate co-precipitation method. hnRNPA1-GFP-LV and NC-GFP-LV were transfected into Lenti-X 293T cells. The culture medium was collected and centrifuged at low speed (800xg, 10 minutes) to remove cell debris and cellular residues. The supernatant was filtered through a 0.45 μm membrane. Virus particles were pelleted from the supernatant using ultracentrifugation (25,000 rpm, 2 hours) and resuspended in PBS. The pellet containing virus particles was filtered through a 0.45 μm membrane. Virus particles were purified using density gradient centrifugation and viral titers were determined. HT-29 and HCT116 cell lines were separately seeded in 24-well plates and cultured until reaching a yield of 70% to 80%.

Preparation: hnRNPA1-GFP-LV and NC-GFP-LV were mixed in the specified ratio and subjected to a DMEM culture medium.

Pre-transfection: the pre-treated mixture was slowly dropwise applied to cells. After 24 hours, the culture medium was replaced. The cells were further cultured for 48 hours before the formal transfection was performed.

Formal transfection: hnRNPA1-GFP-LV and NC-GFP-LV were separately applied to the culture medium containing 5 μg/mL polybrene and slowly dropwise applied to cells. After 24 hours, the culture medium was replaced and an appropriate amount of selection drug was applied. The cells were further cultured for 72 hours, and the growth of green fluorescent protein was visualized to assess its viability. Prior to formal transfection, the cell density of groups E and C needed to be adjusted to an appropriate concentration. The temperature of cells during transfection was maintained between 32°C and 37°C. The cells were cultured to a density of over 80% before pre-transfection. Subsequently, the pre-transfection viral supernatant was filtered and centrifuged to remove cellular residues. An appropriate amount of DMEM/F12 culture medium was applied, and the viral suspension was diluted to an

appropriate concentration (MOI=5-10) and applied to the cultured cells. After transfection, cells were incubated in a constant temperature incubator at 37°C and 5% CO_2 for at least 72 hours. After 72 hours, the EP of green fluorescent protein was visualized, and the transfected cells were examined under a microscope to assess their phenotype, including cell morphology and proliferation status. The collected cells were divided into two groups, with one group cultured in a complete medium containing hygromycin for two weeks for subsequent *in vivo* tumorigenesis experiments, and the other group of cells cultured normally for other experiments.

Detection of hnRNPA1 mRNA EP in two groups of cells

RT-qPCR technology was utilized to detect the EP of hnRNPA1 mRNA in two groups of cells. Firstly, total RNA was extracted using the Trizol method. That is, 1 mL of Trizol reagent was applied to the culture dish, and the reagent was thoroughly mixed and wetted all cells using a pipette. The culture dish containing Trizol was placed at 25°C and allowed to stand for 5 minutes to completely lyse cells with Trizol. The Trizol mixture was transferred to a centrifuge tube using aseptic techniques. A total of 200 μL of soluble guanidine salt buffer was applied and thoroughly mixed with the sample, then left to stand at 25°C for 5 minutes. Then, 500 μL of sterile DEPC-treated water was supplemented and thoroughly mixed. The mixture was transferred to a sterile RNase-free filter tube, and impurities such as cell debris, DNA, lipids, and proteins were pelleted by centrifugation (12,000xg, 10 minutes). The supernatant was collected from the filter tube, mixed with 1 mL of 75% ethanol, and centrifuged (7,500xg, 5 minutes) to precipitate the RNA. The supernatant was removed, 1 mL of 75% ethanol was applied, and the RNA was precipitated again by centrifugation (7,500xg, 5 minutes). The supernatant was removed, and the RNA precipitate was transferred to a clean centrifuge tube using a micropipette. An appropriate amount of DEPC-treated water was utilized to fully dissolve the RNA precipitate, creating an RNA solution. The purity of the extracted RNA was assessed using a spectrophotometer, represented by the OD_{260}/OD_{280} ratio. The RNA concentration was determined by the formula: RNA concentration (μg/μL) = OD_{260} × 40 × dilution factor / 1000. The extracted RNA was utilized for subsequent experiments or stored at -80°C to prevent RNA degradation.

After extracting total cellular RNA, a reverse transcription reaction was performed to synthesize cDNA. The reaction system was prepared as follows: 2×RT Master Mix (10 μL), RNA sample (2 μL), RNase-free H_2O (8 μL). The reaction mixture was prepared according to the above proportions, mixed thoroughly, and briefly centrifuged with the tube lid closed. The reaction tubes were placed in a PCR machine, and the reaction conditions were set as follows: 35°C for 15 minutes, 85°C for 5 seconds, and 30 cycles at 4°C. After the reverse transcription reaction, the cDNA was either stored at a cold temperature or frozen

Table 1. Reaction system.

Component	Volume (μL)
SYBR Green I	10
RNase-free H_2O	X
Forward primer (10 μM)	1
Reverse primer (10 μM)	1
cDNA	2

for future use. Next, RT PCR (SYBR Green I dye method) was performed to amplify the hnRNPA1 gene and the reference gene GAPDH. The reaction system was prepared according to the proportions shown in Table 1.

The synthesis of primers for hnRNPA1 and the reference gene GAPDH was performed by Jiangsu Genecefe Biotechnology Co., Ltd. The primer sequences can be found in Table 2. Regarding the reaction conditions, a pre-denaturation step at 95°C for 30 seconds was performed, followed by 46 amplification cycles, each consisting of denaturation at 95°C for 5 seconds and annealing at 60°C for 30 seconds to amplify the hnRNPA1 gene and the reference gene GAPDH. Subsequently, an annealing step at 95°C for 15 seconds and 60°C for 1 minute was performed, followed by a melting curve analysis at 93.5°C for 0.5 seconds. The entire experiment was repeated thrice, and the relative EP level of hnRNPA1 was calculated using the $2^{-\Delta\Delta Ct}$ method with GAPDH as the reference gene. Data analysis was performed accordingly.

The reaction mixture was mixed thoroughly and briefly centrifuged with the tube lid closed. The reaction tubes were placed into an RT PCR instrument, and the reaction conditions were set. The instrument started to monitor the real-time changes in fluorescence signals during the PCR amplification process. The EP levels of hnRNPA1 and GAPDH were determined by analyzing the amplification curves and the intensity of fluorescence signals.

Detection of hnRNPA1 protein EP in two groups of cells

RIPA buffer was mixed with phosphatase inhibitors and protease inhibitors. The mixture was shaken on ice for 30 minutes and then centrifuged at 12,000 rpm to collect the supernatant. The protein concentration in cell lysate was determined using a BCA assay kit. Equal amounts of protein samples were taken and mixed with a loading buffer, followed by electrophoresis on an SDS-PAGE gel. The proteins in the gel were transferred onto a PVDF membrane. The membrane was blocked with 5% skim milk in TBST buffer to prevent nonspecific binding. The membrane was then incubated with the primary antibody, hnRNP A1, at 25°C for 2 hours. After incubation, the membrane was washed thrice with TBST buffer for 5 minutes each. Next, a horseradish peroxidase-conjugated secondary antibody was applied and incubated at 25°C for 1 hour. The membrane was washed again thrice with TBST buffer for 5 minutes each. Finally, an ECL substrate was utilized for exposure and development, and the image was captured with a camera. Western blot images were analyzed

Table 2. Primer sequences.

Primer	Upstream sequence	Downstream sequence
hnRNPA1	5'-TCTGCTGAGGACTGCTGGAA-3'	5'-TCTGCTGAGGACTGCTGGAA-3'
GAPDH	5'-GAAGGTGAAGGTCGGAGT-3'	5'-GAAGATGGTGATGGGATTTC-3'

using software such as Image J to calculate the relative EP level of the hnRNP A1 protein.

Plate clone formation experiment

The cells in two groups with a good growth status were digested with 0.25% trypsin and mechanically dissociated into a single-cell suspension. The single cells were seeded into a 6-well plate. After cell seeding, the 6-well plate was placed in a cell culture incubator under conditions of 37°C, 5% CO_2, and 95% humidity. After a certain period of cultivation, the 6-well plate was removed. The culture medium was aspirated, and cells were washed once with PBS. Then, 4% paraformaldehyde was applied for fixation, and the plate was kept at 25°C for 10-15 minutes. After removing the fixation solution, 0.1% Prussian blue staining solution was utilized. The plate was incubated at 25°C for 15-20 minutes, followed by washing to remove the staining solution. The plate was rinsed thrice with running water and allowed to air dry. The cells were then observed and counted under a high-power microscope. The experiment was repeated thrice, and the number of formed colonies and the colony formation rate were recorded and analyzed.

Detection of tumor stem cell surface markers in two groups

Two groups of cells in good growth condition were digested using 0.25% trypsin and dissociated into single-cell suspension. The surface markers CD133 and CD44 were detected. The cells were suspended in 500 µL PBS at a concentration of 1×10^6 cells/mL. Then, 5 µL of CD133-FITC antibody and CD44-PE antibody were applied separately and incubated for 20 minutes at 25°C with gentle mixing. The cells were washed once with 500 µL PBS, centrifuged at 1,500 rpm for 5 minutes, and the supernatant was discarded. This washing step was repeated twice, and cells were resuspended in 500 µL PBS. Flow cytometry was utilized for detection, and the data were recorded and analyzed. The experiment was repeated thrice, and the results were expressed as the average values.

Tumor formation experiment in mice

Ensuring the selected mice were in good health condition, cells were injected into the mice subcutaneously to initiate tumor formation. The injection site of the mice was observed periodically to monitor the presence of tumors, and observations were recorded until the end of the experiment. After euthanizing the mice, tumor samples were collected for further experimental analysis. Based on the collected tumor samples, the tumor volume was calculated using $V = (L \times W^2)/2$. Here, *V* represents the tumor volume, *L* represents the longest diameter of the tumor, and *W* represents the shortest diameter of the tumor.

Cell invasion experiment, scratch experiment, and CCK-8 experiment

Cell invasion assay was as follows. The lower chamber of a 24-well Transwell plate was pre-filled with DMEM medium containing 10% fetal calf serum (FBS) and placed in a 37°C incubator for preheating. The upper chamber of the Transwell was filled with DMEM medium containing 0.1% BSA, and the chamber was placed in a 37°C incubator for preheating. Cells from the two groups were cen-

trifuged and collected and then resuspended in DMEM medium containing 0.1% BSA. The cell concentration was measured and adjusted to the same density. The DMEM medium in the lower chamber of the Transwell was aspirated and replaced with an equal volume of DMEM medium containing 10% FBS. The cell suspensions of the two groups were applied to the upper chamber of the Transwell, and the Transwell was placed in a 24-well plate containing DMEM medium with 10% FBS. The 24-well plate was incubated in a constant temperature incubator at 37°C with 5% CO_2 for 24 hours. After incubation, the Transwell was removed, and cells in the upper chamber were wiped off with a cotton swab, while cells in the lower chamber were fixed with 4% paraformaldehyde. The cells in the lower chamber were stained with 0.1% crystal violet, the excess staining solution was removed, and the cells were cleaned with a washing solution. Finally, the Transwell was taken out, the filter membrane was cut and placed on a glass slide, and the invaded cells were observed and counted under a microscope.

Scratch assay was as follows. A 1 mL serum-free DMEM medium was applied to the bottom of a cell culture dish where cells were growing. Using a pipette tip, a straight line was made to create a scratch on the cell monolayer. The cells in the dish were cleaned with PBS to remove cell debris and culture medium, and then DMEM medium was added. The dish was placed in a 37°C, 5% CO_2 incubator for 24 hours. After incubation, cells were cleaned with PBS to remove the culture medium and then fixed with 4% paraformaldehyde. The cells were cleaned with PBS and fixed with ethanol. Finally, cells were stained with a fluorescently labeled antibody, and cell migration was visualized under a microscope.

CCK-8 assay was as follows. Cells were digested with 0.25% trypsin and dissociated into single-cell suspension. The cells were then uniformly seeded into each well of a 96-well plate according to the desired cell density. The plate was placed in a CO_2 incubator and cells were incubated at 37°C with 5% CO_2 and 95% humidity. At different time points (24 h, 48 h, 72 h), cells from the two groups were treated with 10 µL of CCK-8 reagent and incubated at 37°C for 1-4 hours. After incubation, the absorbance was measured, and the absorbance values of each well were recorded for data processing. The absorbance values of the two groups at each time point were subtracted to obtain the corresponding relative proliferation rate, and a growth curve was plotted based on these values.

Detection of protein EP of key indicators of Wnt/β-catenin pathway

Western blot technology was still utilized for detection, and detection indicators included protein EPs of β-catenin, Axin2 and Cyclin D1. Please refer to Section 2.5 for experimental steps.

Statistical analysis

All the experiments mentioned above were repeated thrice, and the results were averaged and presented as mean±standard deviation. Data analysis was performed using SPSS 22.0, and a paired t-test was utilized to compare data between groups. *P*<0.05 was taken as statistically significant.

Results

Detection of OP effect of hnRNPA1

In Figure 1A, the relative EP of hnRNPA1 in group E (3.48±0.56) of HT-29 cells was substantially superior to that in group C (0.95±0.28) ($P<0.05$). Similarly, in HCT116 cells, the relative EP of hnRNPA1 in group E (3.29±0.47) was also markedly superior to that in group C (0.97±0.35) ($P<0.05$).
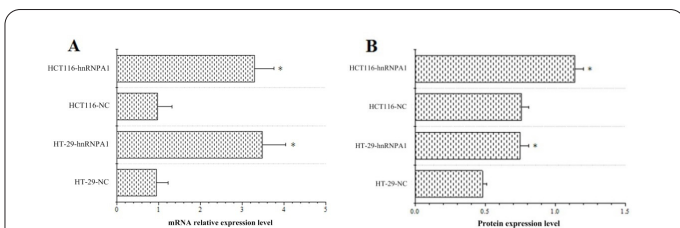
In Figure 1B, the protein EP of hnRNPA1 in group E of HT-29 cells (0.75±0.06) was drastically superior to that in group C (0.48±0.03) ($P<0.05$). Similarly, in HCT116 cells, the protein EP of hnRNPA1 in group E (1.14±0.06) was higher versus group C (0.76±0.05) ($P<0.05$). Hence, the OP of hnRNPA1 in cells was notable, confirming the successful experimental modeling.
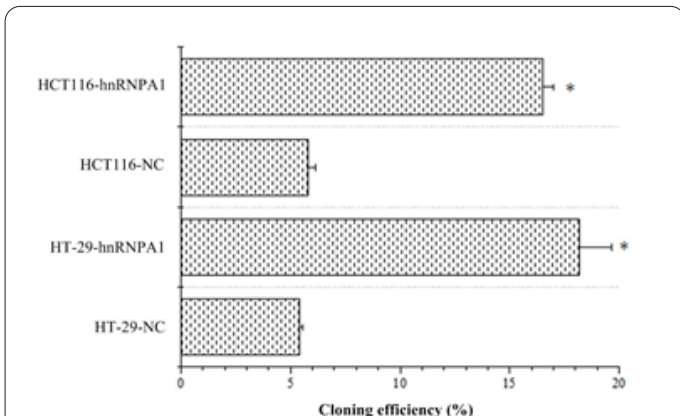
Comparison of cell colony formation ability

In Figure 2, the detection results revealed that the clone formation rate of group E cells in the HT-29 cell line (18.2±1.45%) was remarkably superior to that of group C (5.4±0.18%) ($P<0.05$). Similarly, in the HCT116 cell line, the clone formation rate of group E cells (16.5±0.48%) was higher versus group C (5.8±0.34%) ($P<0.05$). The colony formation ability of group E cells was markedly higher than that of group C.

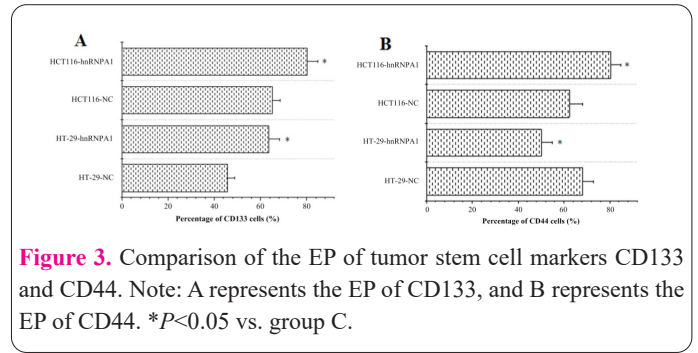### EP comparison of tumor stem cell markers CD133 and CD44

In Figure 3, group E cells in the HT-29 cell line exhibited a considerably superior percentage of CD133-positive cells (63.6±4.7%) versus group C (45.8±3.1%), and a greatly higher percentage of CD44-positive cells (68.3±4.5%) relative to group C (50.2±4.8%) ($P<0.05$). Similarly, in HCT116 cells, group E cells showed a


Figure 1. Detection of hnRNPA1 OP effects. Note: A represents the relative EP levels of hnRNPA1, while B represents the protein EP of hnRNPA1. *$P<0.05$ vs. group C (for Figures 1-6).

Figure 2. Comparison of cell colony formation ability. Note: *$P<0.05$ vs. group C.

Figure 3. Comparison of the EP of tumor stem cell markers CD133 and CD44. Note: A represents the EP of CD133, and B represents the EP of CD44. *$P<0.05$ vs. group C.
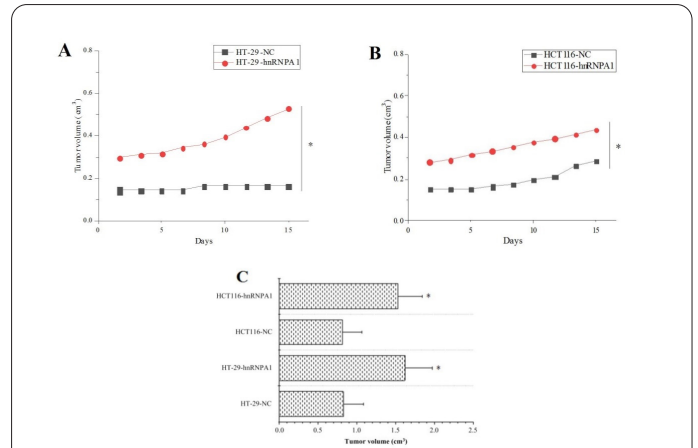
Figure 4. Comparison of tumorigenic capacities in two cell groups. Note: A represents the growth curve of HT-29 cells, B represents the growth curve of HCT116 cells, and C represents the volume of excised tumors in both groups. *$P<0.05$ vs. group C.

drastically higher percentage of CD133-positive cells (80.2±4.6%) relative to group C (65.1±3.5%), and a greatly higher percentage of CD44-positive cells (80.6±4.3%) versus group C (62.4±5.7%) ($P<0.05$).

Comparison of tumorigenic capacities in two cell groups *in vitro*

The growth of tumors in the mouse model was observed (Figure 4). After OP of the hnRNPA1 gene in HT-29 and HCT116 cells, the growth rates were notably faster than group C ($P<0.05$). After sacrificing the mice, the volume of the excised tumors was measured. In HT-29 cells, the tumor volume in group E (1.617±0.35 cm³) was observably larger than group C (0.823±0.26 cm³) ($P<0.05$). In HCT116 cells, the tumor volume in group E (1.528±0.31 cm³) was greatly larger than group C (0.814±0.25 cm³) ($P<0.05$).

Comparison of changes in invasive, migratory, and proliferative abilities between two cell groups

In Figure 5, group E in HT-29 cells exhibited a drastically superior number of cells crossing the Transwell chamber (321±10.5) versus group C (64±4.6) ($P<0.05$). Similarly, in HCT116 cells, group E showed a drastically superior number of cells crossing the Transwell chamber (292±8.3) versus group C (50±4.8) ($P<0.05$). The invasive ability of group E cells was notably higher versus group C.

In Figure 5B, group E in HT-29 cells exhibited a dramatically higher scratch closure rate (20.4±0.8%) versus group C (2.18±0.7%) ($P<0.05$). Similarly, in HCT116 cells, group E showed a dramatically higher scratch closure rate (39.2±0.6%) versus group C (6.3±0.7%) ($P<0.05$). The migratory ability of group E cells was notably higher
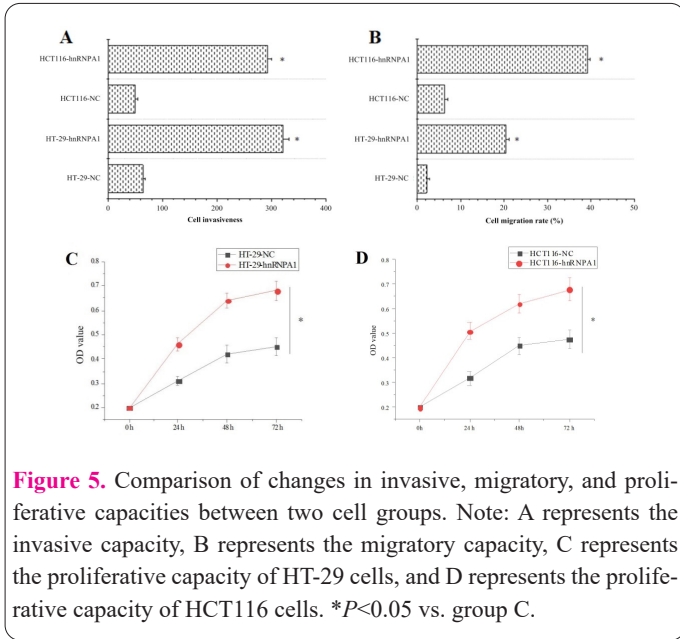
Figure 5. Comparison of changes in invasive, migratory, and proliferative capacities between two cell groups. Note: A represents the invasive capacity, B represents the migratory capacity, C represents the proliferative capacity of HT-29 cells, and D represents the proliferative capacity of HCT116 cells. *$P<0.05$ vs. group C.

versus group C.

In Figure 5C, group E in HT-29 cells exhibited significantly higher optical density (OD) values at 24 h, 48 h, and 72 h (0.46 ± 0.028, 0.64 ± 0.031, 0.68 ± 0.041) versus group C (0.31 ± 0.019, 0.42 ± 0.035, 0.45 ± 0.036) ($P<0.05$). Similarly, in HCT116 cells, group E showed significantly higher OD values at 24 h, 48 h, and 72 h (0.51 ± 0.035, 0.62 ± 0.036, 0.68 ± 0.045) versus group C (0.32 ± 0.028, 0.45 ± 0.033, 0.48 ± 0.037) ($P<0.05$). This indicates that group E cells exhibited markedly superior proliferative capacity versus group C.

Comparison of protein EP in the Wnt/β-catenin signaling

Using GAPDH as an internal reference, it was determined that in HT-29 cells, group E exhibited markedly superior protein EP of β-catenin, Axin2, and Cyclin D1 (0.58 ± 0.05, 0.85 ± 0.06, 0.96 ± 0.07) versus group C (0.34 ± 0.03, 0.31 ± 0.02, 0.42 ± 0.05) ($P<0.05$). For HCT116 cells, group E showed markedly superior protein EP of β-catenin, Axin2, and Cyclin D1 (0.67 ± 0.05, 0.94 ± 0.06, 1.15 ± 0.08) versus group C (0.4 ± 0.04, 0.53 ± 0.05, 0.31 ± 0.06) ($P<0.05$). This indicates that Wnt/β-catenin signaling can be activated by OP of the hnRNPA1 gene
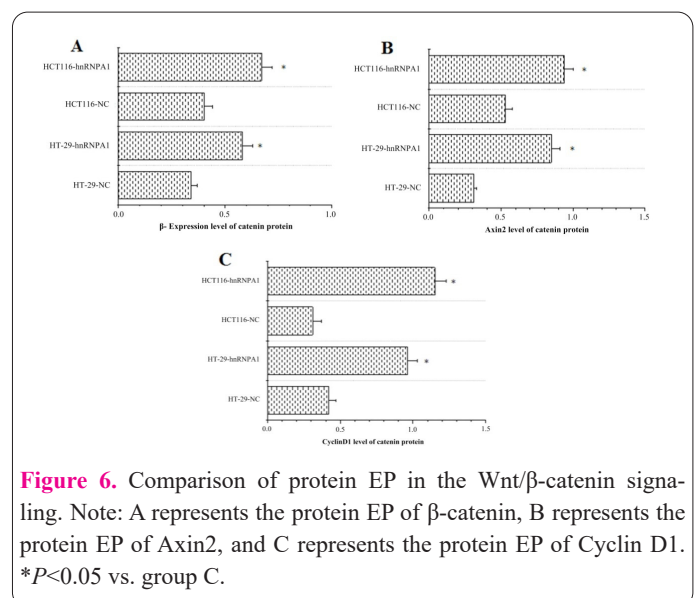
(Figure 6).

Discussion

Intestinal cancer is a highly malignant tumor with limited treatment efficacy, highlighting the significance of exploring the molecular mechanisms underlying its occurrence and development. hnRNPA1 is an RNA-binding protein that plays various roles in cellular processes, including mRNA processing, transport, and translation. Recent studies have indicated abnormal expression of hnRNPA1 in tumor cells and its involvement in processes such as proliferation, invasion, and metastasis (17,18). Therefore, an in-depth investigation of the role of hnRNPA1 in intestinal cancer cells holds promise for providing new insights and approaches for its treatment. In this study, the intestinal cancer cell lines HT-29-hnRNPA1 and HCT116-hnRNPA1 were established as experimental groups, while

HT-29-NC and HCT116-NC were set as control groups. Multiple detection techniques were employed to explore the impact of hnRNPA1 overexpression on cellular proliferative capacity and its influence on the expression of tumor stem cell markers.

Based on the results of hnRNPA1 mRNA EP and hnRNPA1 protein EP detection, successful cell modeling was confirmed. According to the results of colony formation assays, group E of HT-29 and HCT116 cells exhibited notably higher colony formation rates versus group C, indicating a stronger colony formation ability in group E. Colony formation assay is an imperative experiment for evaluating tumor cell proliferation and growth capacity, suggesting that the high EP of hnRNPA1 in group Es promotes cell proliferation and growth. Nevertheless, it should be noted that colony formation assay only reflects the proliferation and growth capacity of cells *in vitro* and may not fully represent the tumor formation ability of cells *in vivo*. Further, *in vivo* experiments are needed to validate the results. Hence, in this work, *in vivo,* tumor formation experiments were conducted using mice to observe the growth of tumors in the mouse models. The results demonstrated that both HT-29 and HCT116 cells with hnRNPA1 gene OP exhibited faster growth rates versus group C. Measurement of the volume of *ex vivo* tumors revealed that in both HT-29 and HCT116 cells, group E exhibited observably larger tumor volumes versus group C. This experimental result indicated that the OP of hnRNPA1 can increase the growth rate and volume of tumors formed by HT-29 and HCT116 cells in mice, implying that hnRNPA1 may play a role in the proliferation and growth of intestinal cancer cells. In the experiment, with the OP of the hnRNPA1 gene in cells, there was an accelerated tumor growth rate and increased tumor volume. This could be attributed to hnRNPA1 potentially regulating multiple downstream signalings, promoting cell proliferation, and reducing cell apoptosis through various mechanisms, thereby enhancing the growth capacity of tumor cells. Liu et al. (19) also mentioned in their study that a contrast of amino acid sequences of HNRNPA1 and HNRNPA2 revealed a high degree of homology in key functional domains. Transfection results indicate that the homologous counterparts, HNRNPA1 and HNRNPA2, regulate each other's EP in a compensatory manner at RNA and protein levels. Furthermore, HNRNPA1 and HNRNPA2 do not affect the

Figure 6. Comparison of protein EP in the Wnt/β-catenin signaling. Note: A represents the protein EP of β-catenin, B represents the protein EP of Axin2, and C represents the protein EP of Cyclin D1. *$P<0.05$ vs. group C.

splicing of their genes. This compensatory degradation is mediated by 3'UTRs of both genes rather than by promoters. This novel regulatory mechanism of HNRNPA1 and A2 EP, through compensatory regulation, tightly controls their EP levels within a certain range to maintain normal cellular activities under various physiological conditions. These findings may provide new targets and insights for intestinal cancer treatment. Further investigation into the role of hnRNPA1 in intestinal cancer progression could help identify new therapeutic targets and drugs.

Tumor stem cells are a subpopulation with self-renewal and differentiation capabilities that can drive tumor growth and metastasis. In this work, the EP of surface markers for tumor stem cells was evaluated in two groups. The results demonstrated that group E of HT-29 and HCT116 cells exhibited a markedly superior positivity rate for CD133 and CD44 versus group C. CD133 and CD44 are known surface markers of tumor stem cells, which exhibit highly invasive and chemoresistant biological properties. They play a crucial role in tumor initiation, growth, and metastasis. Hence, the detection of tumor stem cells holds remarkable importance in tumor diagnosis and treatment. These experimental findings indicated a higher proportion of tumor stem cells in group E cells. This suggests that OP of hnRNPA1 may lead to an increase in tumor stem cells within intestinal cancer cells. This observation is consistent with the previous results from colony formation assays, indicating that hnRNPA1 OP potentially enhances the proliferation and invasive capacity of intestinal cancer cells, thereby promoting the formation and expansion of tumor stem cells. Subsequently, cell invasion assays, scratch assays, and CCK-8 assays were performed on the two cell groups. The results revealed that in HT-29 and HCT116 cells, group E exhibited a drastically superior number of cells invading the chamber versus group C. Moreover, group E demonstrated a superior migration rate in the scratch assay versus group C. Additionally, ODs of group E at 24 h, 48 h, and 72 h were notably higher versus those of group C. Cell invasion assays and scratch assays are commonly utilized cell-based techniques to assess the invasive and migratory abilities of tumor cells. The experimental findings of this work indicated that OP of the hnRNPA1 gene greatly promotes the invasion and migration capabilities of intestinal cancer cells. This effect may be attributed to the involvement of hnRNPA1 in various crucial biological processes, such as post-transcriptional regulation, RNA splicing, and RNA transport. Furthermore, the OP of CD133 and CD44, which are markers of intestinal cancer stem cells, suggests a higher proportion of stem cells in group E cells. This may also contribute to the enhanced invasion and migration capabilities observed in group E. The CCK-8 assay is a commonly utilized methodology for cell proliferation detection, which evaluates cell proliferation capacity by measuring cellular metabolic products. The results of this work demonstrated that the OP of the hnRNPA1 gene markedly promoted the proliferation capacity of intestinal cancer cells. This effect may also be associated with the involvement of hnRNPA1 in biological processes such as cell cycle and DNA repair. Nevertheless, it is imperative to note that although these experimental results indicate a significant role of hnRNPA1 in the growth, proliferation, invasion, and migration of intestinal cancer cells, further research is still needed to investigate its molecular mechanisms and its role in intestinal cancer progression.

The Wnt/β-catenin signaling is an imperative cellular signaling that plays a crucial role in cell proliferation, differentiation, apoptosis, cell fate determination, and embryonic development. This signaling has also been extensively studied in intestinal cancer cells (20). In this work, using GAPDH as an internal reference, the protein EP of key indicators in the Wnt/β-catenin pathway was examined. The results showed that in HT-29 and HCT116 cells, group E exhibited markedly superior protein EP levels of β-catenin, Axin2, and Cyclin D1 versus group C. β-catenin is one of the core members of Wnt/β-catenin signaling. In its inactive state, β-catenin is ubiquitinated and degraded. Upon activation, β-catenin is stabilized and translocated into the nucleus, where it participates in transcriptional regulation processes. Axin2 is a downstream gene of Wnt/β-catenin signaling, and its EP is closely associated with the activation level of this pathway. In an activated Wnt/β-catenin signaling, the EP level of Axin2 is upregulated. Cyclin D1 is a cell cycle-regulating protein and is also considered one of the downstream target genes of Wnt/β-catenin signaling in intestinal cancer. The activated Wnt/β-catenin signaling promotes the EP of Cyclin D1 and drives cell cycle progression. Wang et al. (21) also identified the EP of Frizzled-10 (FZD10) in cancer stem cells (CSCs) through RNA sequencing and conducted an analysis. The results indicated that FZD10 activates Wnt/β-catenin to promote self-renewal, tumorigenicity, and metastasis of cancer CSCs. The activation of FZD10-Wnt/β-catenin in cancer CSCs predicts poor prognosis. In the activated Wnt/β-catenin signaling, the EP level of Cyclin D1 is upregulated. The activation of Wnt/β-catenin signaling leads to the accumulation of β-catenin in the cell nucleus, where it binds to TCF/LEF transcription factors, activating the EP of downstream genes, including Cyclin D1. Cyclin D1 is an imperative regulator of the cell cycle, involved in the transition from the G1 phase to the S phase and promoting cell proliferation. Hence, activation of Wnt/β-catenin signaling is often associated with enhanced cell proliferation and tumorigenesis. The results of this experiment demonstrate that OP of the hnRNPA1 gene can promote activation of the Wnt/β-catenin pathway, leading to increased EP levels of key indicators such as β-catenin, Axin2, and Cyclin D1, thereby promoting the growth and proliferation of intestinal cancer cells. This provides an important experimental basis for in-depth study of the pathogenesis of intestinal cancer and finding new treatment strategies.

Conclusion

This work investigated the impact and underlying mechanisms of the hnRNPA1 gene OP on the biological characteristics of intestinal cancer cells. It was demonstrated that hnRNPA1 gene OP markedly promoted proliferation, invasion, migration, and clonogenicity of HT-29 and HCT116 cells, achieved through Wnt/β-catenin pathway activation. Moreover, the hnRNPA1 gene OP showed a positive correlation with the EP of intestinal cancer stem cell markers. Nevertheless, there are limitations in this work, including the focus on only two types of intestinal cancer cells without considering other different types, and the reliance on cell and mouse models for experimental outcomes, necessitating further preclinical and clinical trials for better adoption in clinical practice. Plans will involve studying more types of intestinal cancer cells to gain a comprehensive understanding of the role of the hn-

RNPA1 gene in intestinal cancer. Building upon cell and animal models, further preclinical investigations will be conducted to provide more reliable theoretical support for clinical treatment. In conclusion, this work provides imperative clues to understanding the role of the hnRNPA1 gene in intestinal cancer progression, offering new insights for clinical therapy of intestinal cancer.

Fundings

References

1. Ramadan R, van Driel MS, Vermeulen L, van Neerven SM. Intestinal stem cell dynamics in homeostasis and cancer. Trends Cancer 2022; 8(5): 416-425. https://doi.org/10.1016/j.trecan.2022.01.011

2. Cheung P, Xiol J, Dill MT, Yuan WC, Panero R, Roper J, Osorio FG, Maglic D, Li Q, Gurung B, Calogero RA, Yilmaz ÖH, Mao J, Camargo FD. Regenerative reprogramming of the intestinal stem cell state via hippo signaling suppresses metastatic colorectal cancer. Cell Stem Cell 2020; 27(4): 590-604. e9. https://doi.org/10.1016/j.stem.2020.07.003

3. Zhao Q, Guan J, Wang X. Intestinal stem cells and intestinal organoids. J Genet Genomics 2020; 47(6): 289-299. https://doi.org/10.1016/j.jgg.2020.06.005

4. Yajing Y, Shizhen Z, Xuelian X, Ling T, Xiaoping X, Jingping C. Comparison of the diagnostic value of capsule endoscopy in two positions for esophageal lesions in the elderly. Acta Medica Mediterranea 2019; 6: 3389-3394. https://doi.org/10.19193/0393-6384_2019_6_533

5. Low YH, Asi Y, Foti SC, Lashley T. Heterogeneous nuclear ribonucleoproteins: implications in neurological diseases. Mol Neurobiol 2021; 58(2): 631-646. https://doi.org/10.1007/s12035-020-02137-4

6. Li H, Liu J, Shen S, Dai D, Cheng S, Dong X, Sun L, Guo X. Pan-cancer analysis of alternative splicing regulator heterogeneous nuclear ribonucleoproteins (hnRNPs) family and their prognostic potential. J Cell Mol Med 2020; 24(19): 11111-11119. https://doi.org/10.1111/jcmm.15558

7. Wang J, Sun D, Wang M, Cheng A, Zhu Y, Mao S, Ou X, Zhao X, Huang J, Gao Q, Zhang S, Yang Q, Wu Y, Zhu D, Jia R, Chen S, Liu M. Multiple functions of heterogeneous nuclear ribonucleoproteins in the positive single-stranded RNA virus life cycle. Front Immunol 2022; 13: 989298. https://doi.org/10.3389/fimmu.2022.989298

8. Ghosh M, Singh M. Structure specific recognition of telomeric repeats containing RNA by the RGG-box of hnRNPA1. Nucleic Acids Res 2020; 48(8): 4492-4506. https://doi.org/10.1093/nar/gkaa134

9. Zhou J, Wu Z, Xu H, Gao L, Wang C, Zheng F, Yao Y. Nano-carbon-based application of parecoxib sodium combined with hydromorphone in preventing anesthesia hyperalgesia caused by remifentanil after thyroidectomy. Cell Mol Biol (Noisy-le-grand) 2022; 68(3): 213-220. https://doi.org/10.14715/cmb/2022.68.3.24

10. Li W, He Y, Yang J, Hu G, Lin Y, Ran T, Peng B, Xie B, Huang M, Gao X, Huang H, Zhu H, Ye F, Liu W. Profiling PRMT methylome reveals roles of hnRNPA1 arginine methylation in RNA splicing and cell growth. Nat Commun 2021; 12(1): 1946. https://doi.org/10.1038/s41467-021-21963-1

11. Zheng H, Chen C, Luo Y, Yu M, He W, An M, Gao B, Kong Y, Ya Y, Lin Y, Li Y, Xie K, Huang J, Lin T. Tumor-derived exosomal BCYRN1 activates WNT5A/VEGF-C/VEGFR3 feedforward loop to drive lymphatic metastasis of bladder cancer. Clin Transl Med 2021; 11(7): e497. https://doi.org/10.1002/ctm2.497

12. Liu J, Xiao Q, Xiao J, Niu C, Li Y, Zhang X, Zhou Z, Shu G, Yin G. Wnt/β-catenin signalling: function, biological mechanisms, and therapeutic opportunities. Signal Transduct Target Ther 2022; 7(1): 3. https://doi.org/10.1038/s41392-021-00762-6

13. Zhang Y, Wang X. Targeting the Wnt/β-catenin signaling pathway in cancer. J Hematol Oncol 2020; 13(1): 165. https://doi.org/10.1186/s13045-020-00990-3

14. Liang W, Shi C, Hong W, Li P, Zhou X, Fu W, Lin L, Zhang J. Super-enhancer-driven lncRNA-DAW promotes liver cancer cell proliferation through activation of Wnt/β-catenin pathway. Mol Ther Nucleic Acids 2021; 26: 1351-1363. https://doi.org/10.1016/j.omtn.2021.10.028

15. Wang HX, Wang XY, Fei JW, Li FH, Han J, Qin X. microRNA-23B inhibits non-small cell lung cancer proliferation, invasion and migration via downregulation of RUNX2 and inhibition of Wnt/B-catenin signaling pathway. J Biol Regul Homeost Agents 2020; 34(3): 825-835. https://doi.org/10.23812/20-11-A-34

16. Yin W, Pham CV, Wang T, Al Shamaileh H, Chowdhury R, Patel S, Li Y, Kong L, Hou Y, Zhu Y, Chen S, Xu H, Jia L, Duan W, Xiang D. Inhibition of autophagy promotes the elimination of liver cancer stem cells by CD133 aptamer-targeted delivery of doxorubicin. Biomolecules 2022; 12(11): 1623. https://doi.org/10.3390/biom12111623

17. Lan Z, Yao X, Sun K, Li A, Liu S, Wang X. The interaction between lncRNA SNHG6 and hnRNPA1 contributes to the growth of colorectal cancer by enhancing aerobic glycolysis through the regulation of alternative splicing of PKM. Front Oncol 2020; 10: 363. https://doi.org/10.3389/fonc.2020.00363

18. Fitzgerald D, Laurent M, Funaro M, Harel A, DeAngelis T, Bangeranye C, Najjar S, Tabansky I, Stern JNH. Defining the role of T lymphocytes in the immunopathogenesis of neuromyelitis optica spectrum disorder. Discov Med 2020; 29(157): 91-102.

19. Liu AQ, Qin X, Wu H, Feng H, Zhang YA, Tu J. hnRNPA1 impedes snakehead vesiculovirus replication via competitively disrupting viral phosphoprotein-nucleoprotein interaction and degrading viral phosphoprotein. Virulence 2023; 14(1): 2196847. https://doi.org/10.1080/21505594.2023.2196847

20. Liao H, Li X, Zhao L, Wang Y, Wang X, Wu Y, Zhou X, Fu W, Liu L, Hu HG, Chen YG. A PROTAC peptide induces durable β-catenin degradation and suppresses Wnt-dependent intestinal cancer. Cell Discov 2020; 6: 35. https://doi.org/10.1038/s41421-020-0171-1

21. Wang J, Yu H, Dong W, Zhang C, Hu M, Ma W, Jiang X, Li H, Yang P, Xiang D. N6-methyladenosine-mediated up-regulation of FZD10 regulates liver cancer stem cells' properties and lenvatinib resistance through WNT/β-catenin and hippo signaling pathways. Gastroenterology 2023; 164(6): 990-1005. https://doi.org/10.1053/j.gastro.2023.01.041